



Diphosphonucleotide phosphatase/phosphodiesterase (PPD1) from yellow lupin (*Lupinus luteus* L.) contains an iron–manganese center

Mariusz Olczak*, Justyna Ciuraszkiewicz, Halina Wójtowicz, Dorota Maszczak, Teresa Olczak

Laboratory of Biochemistry, Faculty of Biotechnology, University of Wrocław, Tamka 2, 50-137 Wrocław, Poland

ARTICLE INFO

Article history:

Received 18 August 2009

Revised 31 August 2009

Accepted 9 September 2009

Available online 13 September 2009

Edited by Miguel De la Rosa

Keywords:

Purple acid phosphatase

Diphosphonucleotide phosphatase

Phosphodiesterase

PPD

Fe–Mn center

ABSTRACT

Yellow lupin diphosphonucleotide phosphatase/phosphodiesterase (PPD1) represents a novel group of enzymes. Here we report that it possesses one iron atom and one manganese atom (1:1 molar ratio) per subunit. The enzyme exhibits visible absorption maximum at ~530 nm. Prolonged oxidation of PPD1 leads to loss of the charge-transfer band and catalytic activity, whereas after reduction PPD1 remains active. Replacement of conserved amino-acid residues coordinating metals results in the loss of enzymatic activity. Despite low amino-acid sequence homology of PPD1 to well-characterized ~55-kDa purple acid phosphatases, their overall fold, topology of active center and metal content are highly similar.

© 2009 Federation of European Biochemical Societies. Published by Elsevier B.V. All rights reserved.

1. Introduction

Purple acid phosphatases (PAPs; EC 3.1.3.2) represent a distinct class of unspecific acid phosphatases that contain dinuclear metal in the active site [1]. Their characteristic purple color is due to a charge-transfer transition caused by a tyrosine residue coordinating a ferric ion. The enzymes catalyze the hydrolysis of a broad range of phosphoric acid esters and anhydrides at a pH 5–6 [2]. Plants contain two major types of PAPs: a dimeric form consisting of two polypeptides of ~55 kDa with or without a disulfide bridge [3] and ~35-kDa form homologous to mammalian enzymes [4]. We have purified and characterized two unspecific PAPs from yellow lupin (AP1 and AP2) [5–7] and an enzyme that specifically hydrolyzes diphosphonucleotides and phosphodiesteres (PPD1) [8–11]. The latter belongs to a novel group of enzymes comprising several proteins (PPD1–PPD4). Nucleotide pyrophosphatase/phosphodiesterase (NPP) is a widely distributed enzymatic activity which results in the hydrolytic breakdown of pyrophosphate and phosphodiester bonds of numerous nucleotide-sugars [12–14]. However, PPD1 does not hydrolyze nucleotide-sugars and is the most active against dinucleotides [8].

All known dinuclear metallohydrolases have homodivalent metal centers of the Zn(II)–Zn(II), Fe(II)–Fe(II), or Mn(II)–Mn(II) type [15]. The only exception is a group of PAPs with a confirmed dinu-

clear center composed of Fe(III)–Mn(II). The second metal in plant PAPs is zinc in the red kidney bean enzyme, in the soybean enzyme, and in one of the three known sweet potato isoenzymes [1,16,17], manganese in the second sweet potato isoenzyme [1,18], and iron in the third sweet potato isoenzyme and in tobacco phosphatase [19,20].

The crystal structures of plant PAPs from red kidney bean and sweet potato showed that the respective catalytic domains are formed by two sandwiched β -sheets surrounded by α -helices [2,21–23]. The active center is composed of a characteristic set of seven amino-acid residues involved in the bonding to the dinuclear metallic center. The Fe(III) coordinates to tyrosine, histidine, aspartate residues and a hydroxo/aqua ligand, the divalent metallic center coordinates to two histidine residues, an asparagine and a terminal aqua ligand, and an aspartate residue bridges the two metal ions [22–24].

The aim of this study was to analyze conserved amino-acid residues involved in metal coordination and identify metals in the active site of PPD1. For this purpose, modified method of PPD1 purification was designed and applied.

2. Materials and methods

2.1. Construction and overexpression of recombinant PPD1

Point mutations were introduced using a MultiChange Site-Directed Mutagenesis Kit (Stratagene). PPD1 (EMBL Accession

* Corresponding author. Fax: +48 71 3752 608.

E-mail address: Mariusz.Olczak@biotech.uni.wroc.pl (M. Olczak).

Number AJ421009) lacking the signal peptide sequence was cloned into the pEx-5 vector (Novagen) in frame with the AKH signal peptide sequence [25] and used as a template for mutagenesis. All conserved amino-acid residues [3] with a potential ability to bind metal were substituted with an alanine, resulting in PPD1 protein variants (Table 1). All proteins were overexpressed using direct expression system and *Sf9* cells [25]. For the truncated versions of PPD1, N-terminal 20, 40 or 60 amino-acid residues located immediately after the signal peptide sequence were deleted (Table 1). The truncated DNA sequences were cloned into the pEx-5 vector [25] using restriction enzymes indicated in Table 1. The proteins were secreted outside the cell and analyzed in the culture medium for their catalytic activity against bis-*p*-NPP [10].

2.2. Purification of PPD1 from yellow lupin seeds

Purification of native PPD1 from yellow lupin seeds was carried out as described previously [8] with the following modifications. Ammonium sulfate fractionation was performed with the chemical of the highest purity (Fluka) without incubations after salt additions, followed by dialysis carried out for 6 h only with buffer changes every 30 min. UnoS column (Bio-Rad) instead of the previously used MonoS column (Pharmacia) was applied.

2.3. Metal ion analysis

Electronic absorption spectra were recorded using an Agilent 8453E UV-Vis spectrophotometer (Agilent Technologies). PPD1 (15 μ M subunit concentration) oxidation was carried out by incubating the enzyme in 50 mM acetate buffer, pH 5.0, containing 30 mM H_2O_2 and reduction in the buffer containing 140 mM 2-mercaptoethanol for 1, 24, and 48 h. To identify metal ions, inductively coupled plasma-atomic emission spectroscopy (ICP-AES) was applied using Liberty 220 spectrometer (Varian) with standard pneumatic nebulizer.

2.4. Protein analyses

The protein concentration during purification was determined using the modified Bradford method (Roti-Nanoquant, Roth). The concentration of the purified enzyme was determined using PPD1 absorbance coefficient [8]. Proteins were analyzed using SDS-PAGE and Coomassie Brilliant Blue G-250 staining (CBB) or Western blotting with anti-polyHis antibodies conjugated with horseradish peroxidase (HRP; Sigma) and chemiluminescence staining (Perkin-Elmer).

Table 1

Primers used in this study.

Primer	Sequence	Description
PPD1-D297A	5'-cgtgtgatgatatttgggtgatatgggaaaggcagaagc-3'	gat → gct
PPD1-D338A	5'-gtcttccacatcgggtgacttgtgtctatgctaattgg-3'	gac → gcc
PPD1-Y341A	5'-ccaacatcgggtgacttgtgtctatgctaattggatatttcacag-3'	tat → gct
PPD1-N371A	5'-cctatatgacacagcaagtggcacaacatgagcgtgtaotggc-3'	aac → gcc
PPD1-H460A	5'-ccatggcgtgatatttcttgcacatagagtaacttggttattctctgc-3'	cat → gct
PPD1-H502A	5'-ggacatagccatgtacgggacatgtccataaactacgaaagaac-3'	cat → gct
PPD1-H504A	5'-gcatgtacggacatgtccataaactacgaaagaacatgcc-3'	cat → gct
PPD1-20F	5'-ctgggtctcGGATCCacatgcttatacaaggccactc-3'	Forward primer with Eco31I and BamHI restriction sites
PPD1-40F	5'-ctgggtctcGGATCCagttacgtgcaatatagtaataaac-3'	Forward primer with Eco31I and BamHI restriction sites
PPD1-60F	5'-ctgggtctcGGATCCactgcaaaactcagtgcttc-3'	Forward primer with Eco31I and BamHI restriction sites
PPD1-R	5'-cgggtctcAAGCTTtagatgccaatgtgtgtagttgg-3'	Reverse primer with Eco31I and HindIII restriction sites

Mutation sites are underlined. Eco31I restriction site is shown in italic and BamHI or HindIII restriction sites in capital letters. Eco31I enzyme cleaves within BamHI and HindIII recognition sites resulting in their specific sticky end.

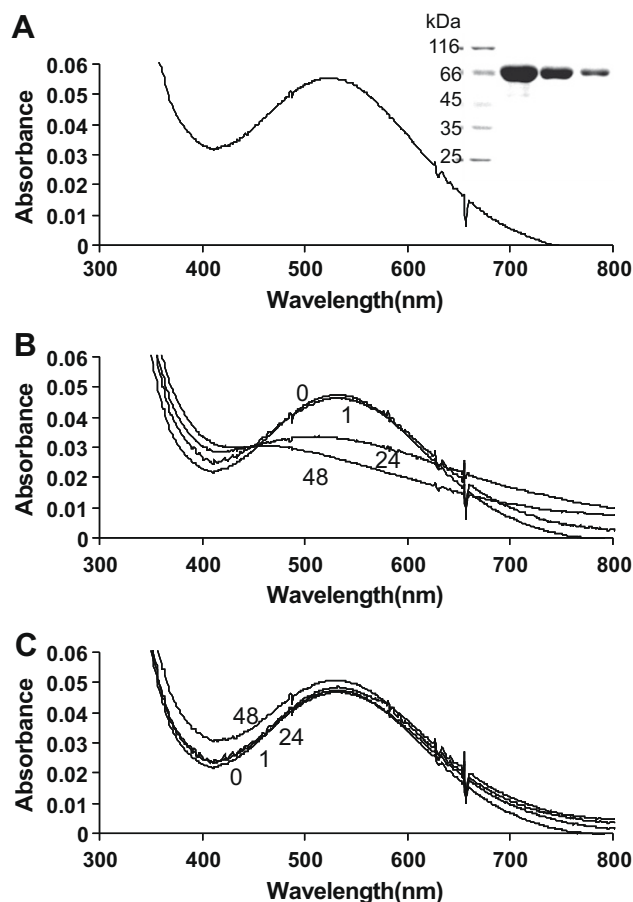


Fig. 1. Visible absorption spectra of PPD1. (A) Spectrum of PPD1 (15 μ M) purified from yellow lupin seeds. The protein was analyzed in 20 mM acetate buffer, pH 5.0, containing 0.4 M NaCl. The inset shows the purified PPD1 (25, 5, and 1 μ g) separated by SDS-PAGE and stained with CBB. Spectra of PPD1 after oxidation with 30 mM H_2O_2 (B) or reduction with 140 mM 2-mercaptoethanol (C). Spectra were recorded before the addition of the appropriate agents (time 0) and after incubation for 1, 24, and 48 h.

2.5. Molecular modeling

The modeling of the 3D structure of PPD1 was performed using a Web-based homology modeling server SWISS-PROT (<http://swissmodel.expasy.org/>). Sweet potato PAP B chain structure (1xzw) [22] was identified as the most appropriate template based on amino-acid sequence identity (27%). The structural alignment was adjusted using DeepView program. The model was refined by homology-based loop building and energy minimization and

its quality was assessed by PROCHECK [26] and Verify3D [27] software. The structure was visualized using VMD 1.6.8 software (<http://www.ks.uiuc.edu/>).

3. Results and discussion

3.1. Spectroscopic characterization of PPD1

Previously, we purified and characterized PPD1 from yellow lupin seeds [8]. However, the protein was unstable in solutions, easily precipitated during storage and concentration, and its solutions were colorless, suggesting that purification process could lead to partial metal loss. Therefore, in this study PPD1 was isolated using modified method. This resulted in the higher stability and activity of the purified enzyme, thus allowing its concentration and color visualization. The purified enzyme exhibited significantly higher phosphodiesterase activity, compared with the previously published data [8]. V_{\max} for bis-*p*-NPP was determined as 194 ± 15 IU per 1 mg of protein, which corresponded to $k_{\text{cat}} = 243 \pm 18 \text{ s}^{-1}$, calculated for one metallic catalytic center. We also found that the protein samples were colored ($\epsilon = 3600 \text{ M}^{-1} \text{ cm}^{-1}$ per subunit), resulting in the broad maximum of absorbance at $\sim 530 \text{ nm}$ (Fig. 1A), which is slightly shifted compared with typical plant PAPs (550–560 nm) [1,16–18]. The Mn-containing sweet potato purple acid phosphatase isolated by Sugiura et al. [28] exhibited a maximum of absorbance at 515 nm ($\epsilon = 1230 \text{ M}^{-1} \text{ cm}^{-1}$ per subunit). This was in contrast to the enzyme characterized by Schenk

et al. [1,18], showing a maximum of absorbance at 560 nm ($\epsilon = 3200 \text{ M}^{-1} \text{ cm}^{-1}$ per subunit). These discrepancies may be explained, at least in part, by different buffer components used by the authors, which might result in partial metal loss. Hefler and Averill [29] and Klabunde et al. [2] reported that PAP from sweet potato and red kidney bean exhibited a maximum of absorbance at 545 nm and 544 nm ($\epsilon = 3080 \text{ M}^{-1} \text{ cm}^{-1}$ and $\epsilon = 3200 \text{ M}^{-1} \text{ cm}^{-1}$ per subunit), respectively, which is more similar to PPD1.

PPD1 oxidation resulted in the loss of both the charge-transfer band (Fig. 1B) and catalytic activity (Fig. 2). However, this effect was observed only after prolonged incubation. It is likely that the loss of enzymatic activity is caused by the oxidation of a conserved tyrosine residue and subsequent release of iron metal [30]. In contrast, reduction of PPD1 did not change the charge-transfer band and catalytic activity (Figs. 1C and 2). All these data demonstrate that PPD1 is an iron-tyrosinate protein typical of the PAPs and requires iron and divalent metal for its enzymatic activity.

3.2. Analysis of PPD1 metallic center

Analysis of metals in the active center demonstrated that PPD1 possesses one iron atom and one manganese atom at a 1:1 molar ratio per subunit (Table 2). The Fe(III)–Mn(II) center is rare among PAPs since it has previously been demonstrated only in one other enzyme, i.e. in one of the isoforms of sweet potato phosphatase [1,18]. By analogy with other PAPs and based on our results (Figs. 1B, C and 2) it seems that the metallic center of PPD1 is active in the form of Fe(III)–Mn(II). This is also confirmed by the report of Schenk et al. [18], showing that dialysis of manganese-depleted

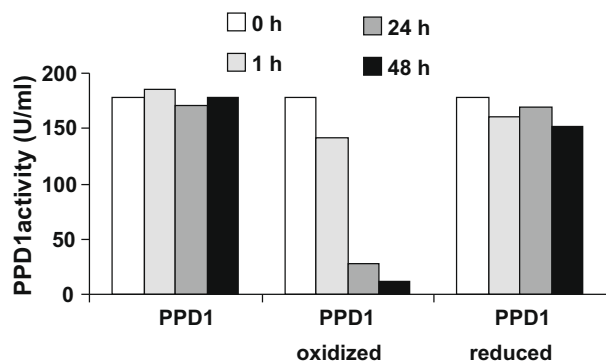


Fig. 2. Catalytic activity of PPD1 purified from yellow lupin seeds after oxidation and reduction. Before and after oxidation with 30 mM H_2O_2 or reduction with 140 mM 2-mercaptoethanol, hydrolytic activity of PPD1 was determined using bis-*p*-NPP as a substrate. Representative data from two independent experiments, resulting in a similar trend, are shown.

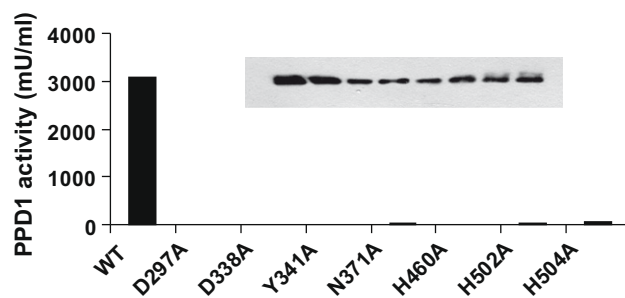


Fig. 3. Catalytic activity of PPD1 protein variants. Recombinant protein variants were overexpressed in directly transfected *Sf9* cells. Protein expression and secretion into the culture medium was analyzed by SDS-PAGE and Western blotting using anti-polyHis antibodies conjugated with HRP and chemiluminescence staining (inset). Hydrolytic activity was determined in the culture medium using bis-*p*-NPP as a substrate.

Table 2
Metal analysis in PPD1.

Preparation	Fe ($\mu\text{g}/\text{nmol}$)	Mn ($\mu\text{g}/\text{nmol}$)	Zn ($\mu\text{g}/\text{nmol}$)	Co ($\mu\text{g}/\text{nmol}$)	Protein ($\mu\text{g}/\text{nmol}$ of subunits)	Fe/protein subunit (mol/mol)	Mn/protein subunit (mol/mol)	Zn/protein subunit (mol/mol)	Co/protein subunit (mol/mol)
1. Sample ^a	0.258/ 4.62	0.295/ 5.27	0.074/ 1.13	bdl	515/6.86	0.67	0.77	0.16	0.0
1. Buffer ^a	bdl ^c	bdl	bdl	bdl					
2. Sample ^b	0.123/ 2.2	0.129/ 2.35	0.002/ 0.0	bdl	235/3.13	0.7	0.75	0.0	0.0
2. Buffer ^b	bdl	bdl	0.002	bdl					
3. Sample ^b	0.679/ 12.16	0.693/ 12.61	0.114/ 1.74	bdl	880/11.7	1.04	1.08	0.16	0.0
3. Buffer ^b	bdl	bdl	0.002	bdl					

^a Protein sample prepared in 50 mM acetate buffer, pH 5.0.

^b Protein samples prepared in 20 mM acetate buffer, pH 5.0, containing 0.4 M NaCl.

^c bdl, below detection level. ICP-AES detection levels calculated for the sample volumes used in this study: Fe = 0.0015 μg , Mn = 0.0003 μg , Zn = 0.001 μg , Co = 0.005 μg . Atomic masses: Fe = 55.85 g/mol, Mn = 54.94 g/mol, Zn = 65.39 g/mol, Co = 58.93 g/mol.

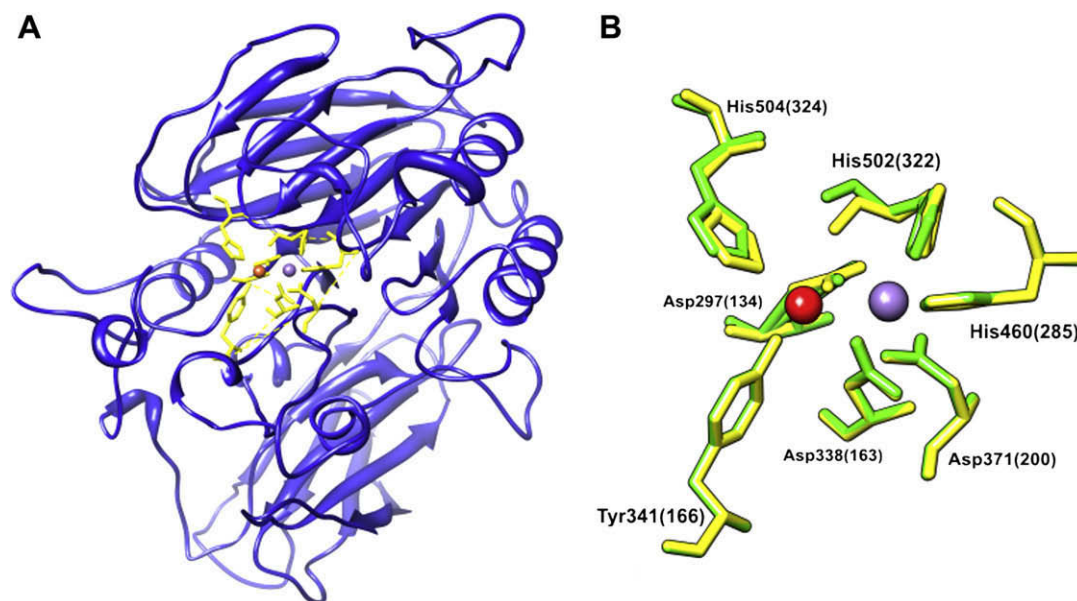


Fig. 4. Homology model of three-dimensional structure of PPD1. (A) The overall view of PPD1 structure (158–602 amino-acid residues) and (B) the overlapped catalytic center of PPD1 and sweet potato PAP (1xzw) [22]. Conserved amino-acid residues of PPD1 and sweet potato PAP are shown in yellow and green, respectively. Iron is shown in red and manganese in purple.

sweet potato PAP in the presence of $MnCl_2$, but not $MnCl_3$, reconstituted enzymatic activity. Our hypothesis is also supported by a general catalytic mechanism of PAPs, which involves coordination of the phosphate ester substrate by the divalent metal ion, followed by nucleophilic attack by a water molecule coordinated to the ferric ion [2,22,23,31,32].

3.3. Importance of conserved amino-acid residues and N-terminal region of PPD1 for catalytic activity

Despite low sequence homology, different subunit arrangements and different metal content, all known PAPs have an almost identical fold of the active-site domain [2,22,23,33]. The active site is composed of invariant amino-acid residues located within five blocks with different number of residues separating the blocks. In PPD1, all five motifs characteristic of PAPs are also conserved [3]. It has been shown that replacement of His202 by an alanine or arginine in red kidney bean PAP caused substantial loss in enzymatic reaction rate and catalytic efficiency [32]. Here we showed that in PPD1, the single replacement of any of the conserved amino-acid residues by alanine resulted in the loss of the enzymatic activity (Fig. 3). Similar experiments performed on typical unspecific PAP from yellow lupin, namely AP1 [5,7], also showed the lack of the hydrolytic activity (data not shown). The replacement of any of the conserved amino-acid residues may result in destabilization of tertiary structure of the active site or removal of essential amino-acid residues required for metal coordination and different steps of catalytic mechanism [20,22,23]. Our data demonstrate that all conserved amino-acid residues of the active center are required for the PPD1 and PAP activity, suggesting that despite low amino-acid sequence homology between these proteins, the mechanism of catalytic mechanism may be similar.

The difference between plant and mammalian PAPs is an additional N-terminal domain of the former [34]. PPD1 contains this N-terminal extension; however, compared with typical ~55-kDa PAPs, the N-terminal sequence of PPD1 is longer (subunit molecular mass ~75 kDa). Therefore, we aimed to analyze whether the N-terminal region is important for PPD1 catalytic activity. However, removal of 20, 40, or 60 amino-acid residues located immediately after the signal peptide sequence resulted in the inhibition of re-

combinant protein secretion to the culture medium, caused probably by improper protein folding. In addition, no PPD1 activity was detected in cell lysates (data not shown). Although it seems that first 60 amino-acid residues of mature PPD1 are important for protein folding, we cannot exclude a possibility that the N-terminal region also contributes to the regulation of enzymatic activity.

3.4. Homology modeling of PPD1 structure

To analyze three-dimensional PPD1 structure, a computational approach was applied. Analysis of amino-acid sequence of PPD1 and sweet potato PAP (EMBL Accession Number AF200825) showed that they share ~450-amino-acid homologous region (158–602 amino-acid residues in PPD1). Within this region, tertiary structures of the proteins are highly similar (Fig. 4A). Moreover, high homology between PPD1 and sweet potato PAP active-site structure was observed with the analogous location of the metal ions coordinating invariant amino-acid residues (Fig. 4B). Only two short regions within PPD1 structure, Asn307–Ser316 and Gln348–Asn357, showed a conformation which remained ambiguous due to low homology to the template and resulted in difficulties in modeling. It is likely that variations in these loops may affect substrate specificities of the respective PAPs.

In conclusion, this is the first report on the characterization of metal center and protein structure of a novel enzyme belonging to PPD group. Despite low amino-acid sequence homology of PPD1 to well-characterized ~55-kDa PAPs, their overall fold, topology of active center and metal content are highly similar.

Acknowledgments

This study was supported by the Grant No. N303 014 32/0670 from the Polish Ministry of Science and Higher Education.

References

- [1] Schenk, G., Ge, Y., Carrington, L.E., Wynne, C.J., Searle, I.R., Carroll, B.J., Hamilton, S. and de Jersey, J. (1999) Binuclear metal centers in plant purple acid phosphatases: Fe–Mn in sweet potato and Fe–Zn in soybean. *Arch. Biochem. Biophys.* 370, 183–189.

- [2] Klabunde, T., Strater, N., Frohlich, R., Witzel, H. and Krebs, B. (1996) Mechanism of Fe(III)–Zn(II) purple acid phosphatase based on crystal structures. *J. Mol. Biol.* 259, 737–748.
- [3] Olczak, M., Morawiecka, B. and Watorek, W. (2003) Plant purple acid phosphatases – genes, structures and biological function. *Acta Biochim. Pol.* 50, 1245–1256.
- [4] Schenk, G., Guddat, L.W., Ge, Y., Carrington, L.E., Hume, D.A., Hamilton, S. and de Jersey, J. (2000) Identification of mammalian-like purple acid phosphatases in a wide range of plants. *Gene* 250, 117–125.
- [5] Olczak, M., Watorek, W. and Morawiecka, B. (1997) Purification and characterization of acid phosphatase from yellow lupin (*Lupinus luteus*) seeds. *Biochim. Biophys. Acta* 1341, 14–25.
- [6] Olczak, M. and Watorek, W. (1998) Oligosaccharide and polypeptide homology of lupin (*Lupinus luteus*) acid phosphatase subunits. *Arch. Biochem. Biophys.* 360, 85–92.
- [7] Olczak, M. and Watorek, W. (2003) Two subfamilies of plant purple acid phosphatases. *Physiol. Plant.* 118, 491–498.
- [8] Olczak, M., Kobialka, M. and Watorek, W. (2000) Characterization of diphosphonucleotide phosphatase/phosphodiesterase from yellow lupin (*Lupinus luteus*) seeds. *Biochim. Biophys. Acta* 1478, 239–247.
- [9] Olczak, M. and Watorek, W. (2000) Structural analysis of N-glycans from yellow lupin (*Lupinus luteus*) seed diphosphonucleotide phosphatase/phosphodiesterase. *Biochim. Biophys. Acta* 1523, 236–245.
- [10] Olczak, M. and Olczak, T. (2002) Diphosphonucleotide phosphatase/phosphodiesterase from yellow lupin (*Lupinus luteus*) belongs to a novel group of specific metallophosphatases. *FEBS Lett.* 519, 159–163.
- [11] Olczak, M. and Olczak, T. (2005) Expression and purification of active plant diphosphonucleotide phosphatase/phosphodiesterase from baculovirus-infected insect cells. *Protein Expr. Purif.* 39, 116–123.
- [12] Rodriguez-Lopez, M., Baroja-Fernandez, E., Zanduetta-Criado, A. and Pozueta-Romero, J. (2000) Adenosine diphosphate glucose pyrophosphatase: a plastidial phosphodiesterase that prevents starch biosynthesis. *Proc. Natl. Acad. Sci. USA* 97, 8705–8710.
- [13] Rodriguez-Lopez, M., Baroja-Fernandez, E., Zanduetta-Criado, A., Moreno-Bruna, B., Munoz, F.J., Akazawa, T. and Pozueta-Romero, J. (2001) Two isoforms of a nucleotide-sugar pyrophosphatase/phosphodiesterase from barley leaves (*Hordeum vulgare* L.) are distinct oligomers of HvGLP1, a germin-like protein. *FEBS Lett.* 490, 44–48.
- [14] Nanjo, Y., Oka, H., Ikarashi, N., Kaneko, K., Kitajima, A., Mitsui, T., Munoz, F.J., Rodriguez-Lopez, M., Baroja-Fernandez, E. and Pozueta-Romero, J. (2006) Rice plastidial N-glycosylated nucleotide pyrophosphatase/phosphodiesterase is transported from the ER-Golgi to the chloroplast through the secretory pathway. *Plant Cell* 18, 2582–2592.
- [15] Wilcox, D.E. (1996) Binuclear metallohydrolases. *Chem. Rev.* 96, 2435–2458.
- [16] Beck, J.L., McConaghie, L.A., Summors, A.C., Arnold, W.N., de Jersey, J. and Zerner, B. (1986) Properties of a purple acid phosphatase from red kidney bean: a zinc-iron metalloenzyme. *Biochim. Biophys. Acta* 869, 61–68.
- [17] Durmus, A., Eicken, C., Sift, B.H., Kratel, A., Kappl, R., Huttermann, J. and Krebs, B. (1999) The active site of purple acid phosphatase from sweet potatoes (*Ipomoea batatas*) metal content and spectroscopic characterization. *Eur. J. Biochem.* 260, 709–716.
- [18] Schenk, G., Boutchard, C.L., Carrington, L.E., Noble, C.J., Moubaraki, B., Murray, K.S., de Jersey, J., Hanson, G.R. and Hamilton, S. (2001) A purple acid phosphatase from sweet potato contains an antiferromagnetically coupled binuclear Fe–Mn center. *J. Biol. Chem.* 276, 19084–19088.
- [19] Kaida, R., Hayashi, T. and Kaneko, T.S. (2008) Purple acid phosphatase in the wall of tobacco cells. *Phytochemistry* 69, 2546–2551.
- [20] Waratrujiwong, T., Krebs, B., Spener, F. and Visoottiviset, P. (2006) Recombinant purple acid phosphatase isoform 3 from sweet potato is an enzyme with a diiron metal center. *FEBS J.* 273, 1649–1659.
- [21] Strater, N., Klabunde, T., Tucker, P., Witzel, H. and Krebs, B. (1995) Crystal structure of a purple acid phosphatase containing a dinuclear Fe(III)–Zn(II) active site. *Science* 268, 1489–1492.
- [22] Schenk, G., Gahan, L.R., Carrington, L.E., Mitic, N., Valizadeh, M., Hamilton, S.E., de Jersey, J. and Guddat, L.W. (2005) Phosphate forms an unusual tripod complex with the Fe–Mn center of sweet potato purple acid phosphatase. *Proc. Natl. Acad. Sci. USA* 102, 273–278.
- [23] Schenk, G., Elliott, T.W., Leung, E., Carrington, L.E., Mitic, N., Gahan, L.R. and Guddat, L.W. (2008) Crystal structures of a purple acid phosphatase, representing different steps of this enzyme's catalytic cycle. *BMC Struct. Biol.* 8, 6.
- [24] Boudalis, A.K., Aston, R.E., Smith, S.J., Mirams, R.E., Riley, M.J., Schenk, G., Blackman, A.G., Hanton, L.R. and Gahan, L.R. (2007) Synthesis and characterization of the tetranuclear iron(III) complex of a new asymmetric multidentate ligand. A structural model for purple acid phosphatases. *Dalton Trans.* 44, 5132–5139.
- [25] Olczak, M. and Olczak, T. (2006) Comparison of different signal peptides for protein secretion in non-lytic insect cell system. *Anal. Biochem.* 359, 45–53.
- [26] Laskowski, R.A., Rullmann, J.A., MacArthur, M.W., Kaptein, R. and Thornton, J.M. (1996) AQUA and PROCHECK-NMR: programs for checking the quality of protein structures solved by NMR. *J. Biomol. NMR* 8, 477–486.
- [27] Luthy, R., Bowie, J.U. and Eisenberg, D. (1992) Assessment of protein models with three-dimensional profiles. *Nature* 356, 83–85.
- [28] Sugiura, Y., Kawabe, H., Tanaka, H., Fujimoto, S. and Ohara, A. (1981) Purification, enzymatic properties, and active site environment of a novel manganese(III)-containing acid phosphatase. *J. Biol. Chem.* 256, 10664–10670.
- [29] Hefler, S.K. and Averill, B.A. (1987) The “manganese(III)-containing” purple acid phosphatase from sweet potatoes is an iron enzyme. *Biochem. Biophys. Res. Commun.* 146, 1173–1177.
- [30] Beck, J.L., Durack, M.C.A., Hamilton, S.E. and de Jersey, J. (1999) Irreversible inactivation of purple acid phosphatase by hydrogen peroxide and ascorbate. *J. Inorg. Biochem.* 73, 245–252.
- [31] Merckx, M., Pinkse, M.W.H. and Averill, B.A. (1999) Evidence for nonbridged coordination for *p*-nitrophenyl phosphate to the dinuclear Fe(III)–M(II) center in bovine spleen purple acid phosphatase during enzymatic turnover. *Biochemistry* 38, 9914–9925.
- [32] Truong, N.T., Naseri, J.L., Vogel, A., Rempel, A. and Krebs, B. (2005) Structure–function relationships of purple acid phosphatase from red kidney beans based on heterologously expressed mutants. *Arch. Biochem. Biophys.* 440, 38–45.
- [33] Klabunde, T., Strater, N., Krebs, B. and Witzel, H. (1995) Structural relationship between the mammalian Fe(III)–Fe(II) and the Fe(III)–Zn(II) plant purple acid phosphatases. *FEBS Lett.* 367, 56–60.
- [34] Tsyguelnaia, I. and Doolittle, R.F. (1998) Presence of a fibronectin type III domain in a plant protein. *J. Mol. Evol.* 46, 612–614.